Jestr

Journal of Engineering Science and Technology Review 16 (6) (2023) 8 - 15

Research Article

JOURNAL OF
Engineering Science and Technology Review

www.jestr.org

The Deformation Response of a Functional Four-Cylinder Reciprocating Engine using Finite Element Analysis and Surrogate Model

Theddeus Tochukwu Akano*, Oladotun Samuel Osasuyi and Harrison Okechukwu Onovo

Department of Mechanical Engineering, University of Botswana, Republic of Botswana

Received 24 May 2023; Accepted 5 November 2023

Abstract

The aim of this study is to examine the deformation response of a four-cylinder reciprocating engine. The model of the engine was done through Autodesk Fusion 360®, while the simulation and analysis were conducted using the finite element analysis backend, Autodesk Nastran solver®. The engine assembly was subjected to a multibody dynamics study as well as a thermodynamic reaction of air-fuel mixture in the cylinder. A connecting rod was examined from the standpoint of component design to see how the maximum stress changed with crankshaft rotation. To start the engine, several crankshaft speeds were used, and the multibody simulation was carried out for 0.16s. The output from the simulation is used as surrogated data for the intelligent system modelling. A considerable degree of agreement was observed between simulation results and predicted values, demonstrating the reliability and accuracy of the model. Furthermore, it was shown that the I-section region of the connecting rod receives the maximum stress for both materials. It is essential to build this area with more strength as a result. The Von Mises stress of AlSiC is consistently lower than its yield strength, at 5.5MPa compared to 43MPa. Aluminum has a Von Mises stress of 3.5MPa, far lower than its yield strength of 276MPa. Both materials had stress levels below their yield strengths, ensuring connecting rod structural integrity. The primary factor influencing the engine's distortion profile and peak values was found to be engine torque. The findings might serve as a springboard for more research and development in this area and advance our understanding of engine behavior.

Keywords: Four-cylinder engine, von Mises stress, torque, mechanical power, element distortion, Autodesk Fusion 360, Autodesk Nastran solver

1. Introduction

Internal combustion engines (ICEs) are thermodynamic engines that start a combustion process by igniting an air-fuel mixture. An internal combustion engine does meaningful work by releasing hot gases directly to the engine's components and rotors, or by pushing on and moving the complete engine [1]. In recent years, improved internal combustion engines have grown in popularity. About 98.9% of all transportation on this planet is currently powered by internal combustion engines [2] and continues to dominate the automobile and commercial vehicle markets. Regardless of the internal combustion engine's current economic and practical advantages, continuous innovation has been required to maintain its supremacy in the transportation market [3]. The most significant source of electricity for the foreseeable future is internal combustion engine technology, which is developing quickly and is efficient, energy-saving, and clean [4].

The ICE utilizes crude oil as its primary source of fuel for power generation. As a result, there is a growing need for crude oil on a daily basis. According to the International Energy Outlook, 2021, as reported by the U.S. Energy Information Administration, the global average daily demand for oil in 2017 amounted to around 97.7 million barrels [5]. According to the world energy balance, the transport sector emerged as the primary consumer of oil, accounting for a significant majority of 56% of global oil consumption[6]. Currently, a plethora of alternative fuels exist that possess the capability to power ICEs. Among the available alternatives, few noteworthy possibilities include biodiesel, compressed natural gas (CNG), liquefied petroleum gas (LPG), biogas, ethanol, methanol, hydrogen, and others. The annual biofuel production reached a volume of 171 billion liters in 2022, and it is projected to see a growth to 182 billion liters by the year 2050. The significance of ICEs within the transportation sector has been discussed in a study conducted by Kalghatgi [7][8]. The technology in question has a long-standing history of over a century, boasting several advantages such as reduced costs associated with both vehicle ownership and maintenance, a notable power to weight ratio, an extended driving range, convenient and efficient refueling capabilities, and a well-established infrastructure.

The structural model must typically be evaluated repeatedly by the model-based approaches, which is a laborious and computationally expensive operation. Conversely, structural applications need the ability to quickly recognize deformation. This problem has prompted researchers to abandon them in favor of data-driven models that are easy to test on a budget. These computationally cheap models are known by a variety of names in literature, such as surrogates, emulators, and metamodels. In addition to structural applications, surrogates have several uses in other scientific disciplines, including uncertainty quantification [9], sensitivity analyses [10], and optimization [11], to shorten model runtimes. Over time, surrogate models have been developed in a variety of areas, including kriging, support vector machines (SVMs), least squares approximation (LSA), and artificial neural networks (ANNs) and response surface models (RSMs). They are frequently created using a data-

*E-mail address: akanott@ub.ac.bw
ISSN: 1791-2377
doi:10.25103/jestr.166.02

driven process that links many independent variables to a set of dependent variables. ANN was used to develop a steel beam in 1989, which is said to be the first time it was published in civil engineering [12]. In recent years, the use of ANNs in civil engineering has grown significantly due to the emergence of big data. As far as we can tell, only a small number of review publications on the use of the machine learning (ML) techniques and ANNs [13]–[17], have discussed the use of ANNs in reciprocating engines.

2. Literature Review

2.1 Studies on ICEs

Attempts to study the sources of thermodynamic heat losses have been ongoing as well as ways to curtail them; mainly through simulations and experiments [18]. Adesina *et al*. [19] studied the delay time and droplet penetration using a global method. The heat transport in the combustion chamber was described by the created model using Annand's correlation. The cylinder pressure and temperature were found to be in good accord with the outcomes of the experiment. Martins *et al*. [20] investigated the effectiveness and emission levels of a typical four-cylinder gas engine with negative valve overlap (NVO). In their study, Kumar [1] focused on the mechanical relationships and engine design of a 3-cylinder engine while analyzing different thermodynamic and multibody assessments. The theoretical findings also supported the simulated results. Xu and Cho [21] conducted laser doppler velocimetry (LDV) used in the in-cylinder flow simulation experiment to determine the velocity field. By creating a computational fluid dynamic (CFD) model for the in-cylinder flow predictions, it was determined that the numerical technique might be altered. The CFD analysis was used by Cheng *et al*. [22] to examine the heavy diesel engine's cylinder head. Both the actual experiment and the temperature distribution on the engine head were precisely in agreement. The result of this work served as a benchmark for the review carried out by Meman *et al*. [23] on the analysis of the cylinder head of the 4-stroke ICEs.

In a related development, Oke *et al*. [24] investigated the issue of heat transmission in spark ignition engines. They developed a model for a 2-stroke spark ignition engine and utilized Comsol Multiphysics® to make predictions about the heat transport and temperature distributions in the combustion chamber. Karayel and Yegin [25] created the prototype of a computer-based torque measuring system that determines if the torque value for the vehicle's front hood hinges was appropriate or not. In a compression ignition engine, Agboola *et al*. [26] investigated the combustion temperature distribution and subsequent heat transmission to the combustion chamber wall. They discovered that combustion temperature distribution and heat transmission to the combustion chamber wall increased with engine speed, peaking shortly after the Top dead center (TDC) and dropping dramatically during the stroke's expansion resulting from the intake and exhaust valves opening and shutting. Selmani *et al*. [27] investigated a conventional piston ring pack for an ICE. Bore distortion orders were employed to evaluate the ring-pack sealing capability in relation to the mass fluxes, inter-ring pressures, and ring dynamics. Ring pack behavior was shown to be influenced by the ordering and amount of bore distortion.

The performance of initially noncircular liners was numerically investigated by Alshwawra *et al*. [28]. Their research demonstrated that a cold-state engine with noncircular liners might dramatically enhance the roundness of the liners in their burned state. In a follow-up research, Alshwawra *et al*. [29] investigated how to improve the conformation of the piston ring-cylinder liner (PRCL) arrangement. Their computational findings reveal an intriguing possibility for friction reduction in internal combustion engines' piston-liner configurations. Similar research was conducted by Zhu *et al*. [30] on the influences of various influencing conditions on the deformation properties of cylinder liners. Their findings might be used to help evaluate and regulate cylinder liner deformation during pre-tightening.

Dorić and Klinar [31] presented the process simulation in a new ICE concept that realizes the variable movement of the piston. The technique was created to achieve a certain motion law that improves the fuel efficiency of ICEs. The verification of the measurement technique, as well as the standardization and linearisation of a detector, were the focus of Popelka's work [32]. Future growth and potential solutions for the problem of direct ignition of combustion in homogeneous charge compression ignition (HCCI) engines were discussed in detail by Mogra and Gupta [33]. As a result, the solution to this challenge in HCCI engines provides a means for making the notion actually usable.

The issue of adjusting the swept volume was investigated by Sroka [34]. In an effort to discover the relationships between the efficiency of the work cycle and engine operating parameters, he defined swept volume by the coefficients governing variations in cylinder diameter and piston stroke. Atre *et al*. [35] carried out the static and buckling analysis of the connecting rod using Ansys. The connecting rod was shown to be capable of withstanding loads up to three times greater than those at present without buckling. Using the same principle, Pathade *et al*. [36] analysed the static load stress analyses of the connecting rod, which was built with material epoxy resin. The results of the maximum stress analysis were verified with mathematical data. Furthermore, Sreeraj *et al*. [37] approximated the design performance on the basis of the constitutive relation and behavior of the cylinder head under different operating conditions. Sathishkumara *et al*. [38] investigated and analysed the stress distribution of pistons at actual engine conditions using two distinct materials of Aluminum Silicon alloys. It was discovered that the piston's upper surface might sustain damage during operating circumstances as a result of temperature. Dharani [39] designed and analysed the appropriate connecting rod and crankshaft bearings for a particular ICE application. The results from the FEA show that the maximum von Mises stress acting on the bearings is below the yield strength of the selected material.

2.2 Artificial Intelligence Integration in ICEs Analysis

As science and technology advance, mechanical engineering transforms from classical mechanical engineering to electro-mechanical and intelligent mechanical engineering. The level of automation and intelligence involve is always improving, expanding into a new stage of growth. As a result, the integration of artificial systems with mechanical and electronic systems has become increasingly important [40]. Intelligent mechanisms have been deployed by various researchers to analyze various behaviours of ICEs. Artificial intelligence (AI) is now widely employed in the identification of mechanical engineering failures [41]–[43]. Fault-based tree, case-based reasoning (CBR) and rule-based reasoning (RBR) are examples of artificial intelligence-based fault diagnosis methodologies [40]. Bhatt and Shrivastava [44]

reviewed the application of ANN to foresee and improve the complex properties of diverse engine types using varied fuels. The ANN model compared well with other prediction models. Researchers are also using machine learning (ML) models to study and regulate complex dynamical systems. These have the potential to transform how we interact with and manipulate them [45]. Machine Learning has been shown to be capable of making accurate predictions of thermo-mechanical and physical properties of components and machines [46]–[52].

In this work, the deformation characteristics of a four-cylinder reciprocating engine is investigated. The model of the four-cylinder engine was done through Autodesk Fusion 360® [53], while the actual simulation and analysis were conducted using the finite element analysis backend, Autodesk Nastran solver® [54]. The engine assembly was subjected to a multibody dynamics study as well as a thermodynamic assessment of the air-fuel mixture in a cylinder. When an air-fuel combination is compressed and burned, it causes a change in pressure inside the combustion chamber. A connecting rod was examined from the standpoint of component design to see how the maximum stress changed with crankshaft rotation.

3. Materials and Methodology

3.1 Modelling and Simulation

A four-cylinder engine was created using Autodesk Fusion 360® and analysed using Autodesk Nastran solver®. All the components of the engine are presumed to be rigid, excluding the two central connecting rod which is flexible, and two material data aluminum and aluminium-silicon-carbon (Al-SiC) alloys were considered. While the other parts are free to move in space, all of the cylinders are fixed. Each piston's upper surface is exposed to the pressure fluctuation that was discovered through thermodynamic research. The engine is started by applying a starting speed of 2000 rpm to the crankshaft, and the multibody simulation was run for 0.16s. The dimensions and parameters of the engine model provided by da Silva *et al*. [55] were utilized. The specifications of the engine are as follows: it has four cylinders, each with a cylinder bore of 86*mm* and a piston stroke of 86*mm*. The connecting rod length measures 160*mm*. The displacement volume of the engine is 500cm^3, while the clearance volume is 28.7cm^3. Lastly, the compression ratio is 18.4:1.

It is a typical procedure to undertake a multibody analysis of an engine while treating each component as a rigid body. The computer-aided design (CAD) designs were modelled using Autodesk Fusion 360, as seen in Fig. 1.

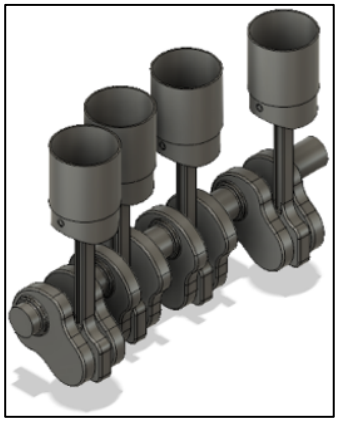

Fig. 1. Geometry of the four-cylinder reciprocating engine

Autodesk Fusion 360 combines computer-aided manufacturing (CAM), structural design, mechanical simulation, and industrial design to create a design mechanism that strengthens cross-platform and cloud collaboration. The visibility of results is a key aspect of direct modelling in Fusion 360. As a result, Autodesk Fusion 360 was used to create the internal combustion engine's piston, connecting rod, and crankshaft assembly.

The mechanical system was simulated and several parameters, such as torque, von Misses stress on the connecting rod, joint force, and element distortion, were analysed using the finite element approach. Furthermore, it was utilized to examine the power produced in relation to the displacement and stress exerted on the mechanical system. This model was used to do a multibody dynamics study of an engine assembly. Both a multibody dynamics study of an engine assembly and a thermodynamic study of an air-fuel combination in the cylinder were taken into consideration. The compression and combustion of the air-fuel combination cause a change in pressure in the combustion chamber. This is calculated using thermodynamics.

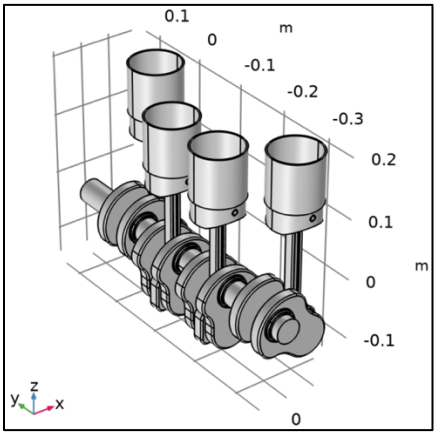

Fig 2. Four-cylinder reciprocating engine system

The torque of the engine and the motion of the engine assembly were calculated using the pressure data from the thermodynamic analysis. Utilizing the Multibody Dynamics interface, this analysis is done. A connecting rod that was examined from the standpoint of component design is modelled. The analysis is done on how this component's maximum stress varies as crankshaft rotates.

3.2 Thermodynamic Analysis

One complete crankshaft rotation is used to calculate the cylinder's pressure change. Figure 3 depicts the geometry that was modelled in this investigation.

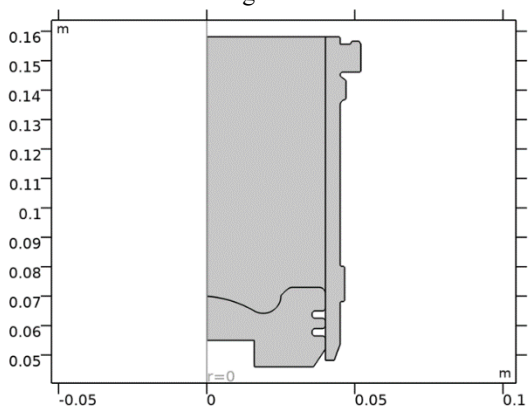

Fig. 3. Axisymmetric view of the piston-cylinder assembly

The heat transfer equations are used to predict the range of temperatures in the cylinder's interior air. In order to take into consideration the rise in temperature brought on by the piston's work, the pressure work is also included. The ideal gas equation is used to simulate the pressure distribution in the air:

$$p = \frac{m}{V}RT \quad (1)$$

where, respectively, $T, \mathrm{V}, p, R\ and\ m$ stand for temperature, volume, pressure, current specific gas constant and mass. As a result of the crankshaft rotation, the piston displacement, x_p, may be expressed as follows:

$$x_p = \sqrt{\sqrt{l^2 - (r_c sin\theta)^2}\ } - r_c cos\theta - (l - r_c) \quad (2)$$

where the terms' r_c, x_p, θ and l and stand respectively for crank radius, piston displacement, crank angle and connecting rod length. It is estimated that each cycle of the crankshaft rotation produces a total energy of 600 *J*.

In the multibody analysis, the engine assembly's motion was controlled by the pressure data that were discovered during the thermodynamic analysis. A crankshaft and four sets of cylinders, pistons, and connecting rods that are comparable to one another make up the engine assembly. A hinge joint secures each piston to the top of a connecting rod, and a prismatic junction links each piston to a cylinder. The bottom ends of all four connecting rods are connected to the same crankshaft via hinged joints. Except for the two central connecting rods and two material data, all engine parts are presumed to be rigid. Aluminum and aluminum-silver-carbon (Al-SiC) alloys were taken into consideration. While the other parts are free to move in space, all of the cylinders are fixed. Each piston's upper surface is subjected to the pressure fluctuation determined by the thermodynamic analysis.

3.3 Application of Artificial Neural Networks in Surrogate Models

In many applications, including system optimization, sensitivity analysis, and design space exploration using surrogate models are playing a bigger role in replacing computationally costly physics-based simulation models. Artificial neural networks (ANNs), one of the fastest-growing fields in machine learning, have been used to model different energy systems.

The ANN model was created using Python® software. The multilayer perceptron (MLP), a feed-forward neural network having one or more layers between input and output layers, was chosen as the neural network's structure. The backpropagation approach, a form of supervised learning, was utilized to train the ANN by providing the correct output response during the training process. Approximately 15% of the cases were selected for the validation test. An additional 15% of the dataset was allocated for training the ANN. Furthermore, another 15% of examples were selected for the purpose of evaluating the effectiveness of the network. These cases were deliberately excluded from the training and validation processes.

The Python® chose cases at random from all of them. Some of the factors taken into account for the input layer in neural network training include torque on the cylinder, maximum stress on the cylinder, mechanical power generated in each cylinder, forces at the connecting rod and crankpin joint, and element distortion of the engine. These characteristics are essential to the training procedure.

4. Results and Discussion

The *p-v* diagram for one of the engine's cylinders, as calculated from the thermodynamic study, is shown in Figure 4. The air-fuel mixture's proportion falls during the combustion cycle, increasing pressure until the piston is nearly at the top dead center (TDC). The combustion starts to take place at this moment, raising the temperature and pressure of the combination in the process. The expansion stroke is then completed when the valve is pushed back toward the bottom dead center (BDC) by highly compressed gas within the cylinder. The pressure of the combination reduces while the process of expansion takes place. The mechanical energy produced throughout a complete crankshaft cycle is represented by the enclosed region in this diagram.

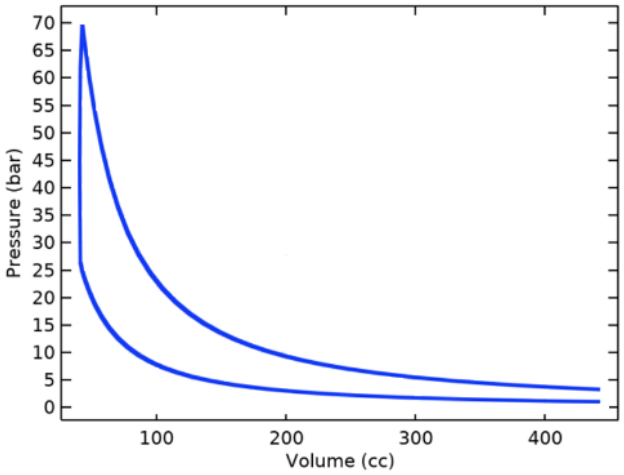

Fig. 4. *p-v* diagram of a cylinder

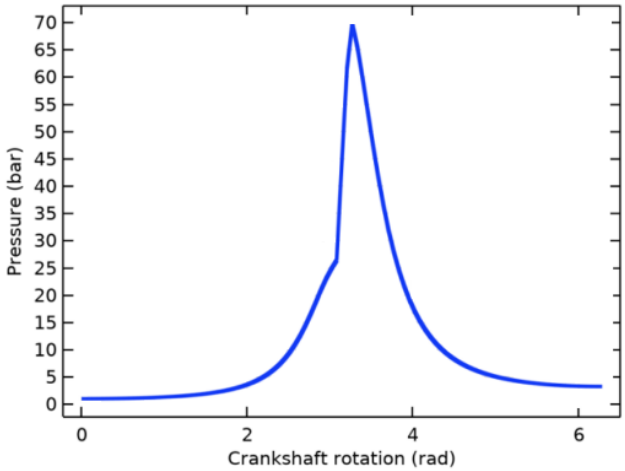

Fig. 5. Variation of the cylinder pressure with the crank rotation

Figure 5 depicts how cylinder pressure fluctuates as a function of crankshaft rotation. The curve is exported and utilized to specify the pressure on the piston's top surface in a multibody analysis. The gas torque is calculated using this pressure of the gas. The stroke, the bore, and the maximum pressure are the variables that determine the graph's form. The ideal Otto cycle, which served as the foundation for the piece-wise function, is what leads to the non-continuous curve. The assumption that the air-fuel combination ignites instantly results in the vertical path at roughly 3 rad.

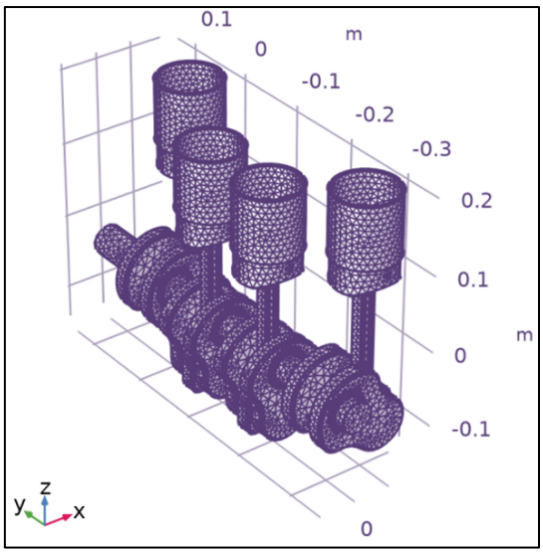

Fig. 6. Mesh representation of the study

The meshing of the assembly is shown below in Fig. 6. Meshing is a very important step in the analysis process. Meshing divides the model into a number of parts for further analysis. If meshing is accurate, then results are also feasible. The finished mesh has more components and degrees of flexibility in the shortest time.

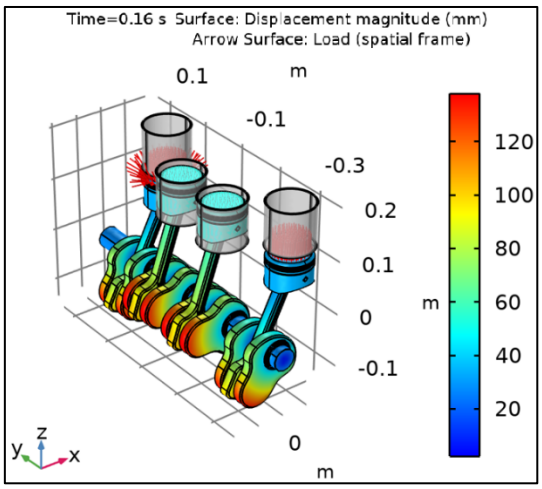

Fig. 7. Displacements of the engine components

Figure 7 depicts the computation of the displacement of several engine parts during the multibody analysis at $t = 0.16$ s. The results of two different materials' stress analysis of the connecting rod are presented in the following section:
(a) Aluminum: The color fluctuation in Figure 8 after 0.16s is used to represent the equivalent stress state distribution across component borders. The connecting rod's minimal stress value is shown by the color blue, while its maximum stress value is shown by the color red. Different colors between blue and red indicate the equivalent stress state intermediate values between the greatest and least equivalent stress. The connecting rod's I-section has the highest value of equivalent stress 3.5×10^6 N/m^2 in this instance, while the connecting rod's minimum value of equivalent stress is approximately 0.1×10^6 N/m^2.

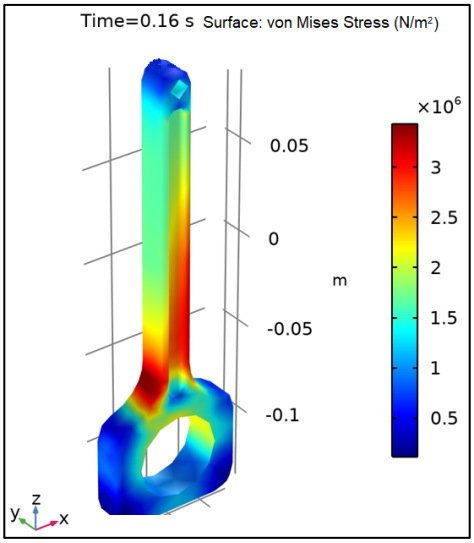

Fig. 8. von Mises stress of Aluminum at 0.16 s.

(b) Aluminum-Silicon-Carbon (AlSiC): The color fluctuation in Figure 9 after 0.16s is used to represent the equivalent stress distribution across the component borders. The connecting rod's minimal stress value is shown by the color blue, while its maximum stress value is shown by the color red. The equivalent stress state between the maximum and minimum are shown by a different color between blue and red. The connecting rod's I-section has the highest value of 5.5×10^6 N/m^2 equivalent stress in this instance, while the connecting rod's minimum value of equivalent stress is approximately 0.1×10^6N/m^2.

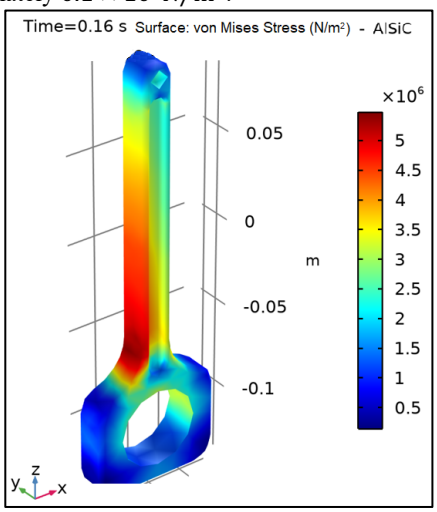

Fig. 9. von Mises stress of Aluminum-Silicon-Carbon (Al-SiC) at 0.16 s

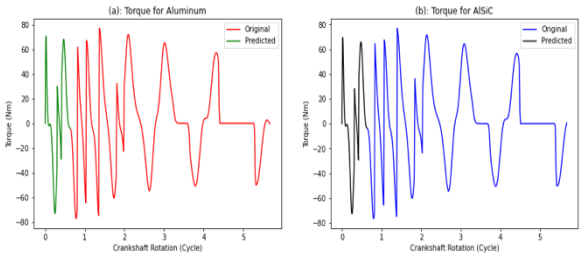

Fig. 10. Torque on the crankshaft at 2000 RPM

Figure 10 shows the engine's rotational force as a function of crank rotation for an engine running at 2000 RPM. It is assumed that the force on the valve and the crank are equal. During the power stroke, the crankshaft's torque is positive; during the compression stroke, it is negative. The variations

in engine torque are brought on by the compression, combustion, and power strokes of an engine's cycle. The power stroke accelerates the crankshaft while the injection pressure contracts the combination of air and fuel in the cavity due to the inertia of the component elements. The Predicted torque of the engine for the two materials considered has two peak torque values within a period of one cycle coinciding with the firing intervals. Since the inertial forces have time to work before the next cylinder is fired, the oscillations are not as smooth and steady.

When the additional power strokes from the initial torque values are taken into account, this behavior may be seen on a minor "plateau." The inconsistent nature of the fuel supply or the circumstances surrounding combustion affects the pressure of the combustion gas in each cylinder, which in turn affects the torque produced by the combustion gas. Thus, the overall torque produced by the combustion of the gas in various cylinders may not be uniform. The instantaneous change of the crankshaft instantaneous angular velocity in the same operating phase interval of each cylinder is caused by the combustion gas torque, which may also have an impact on it.

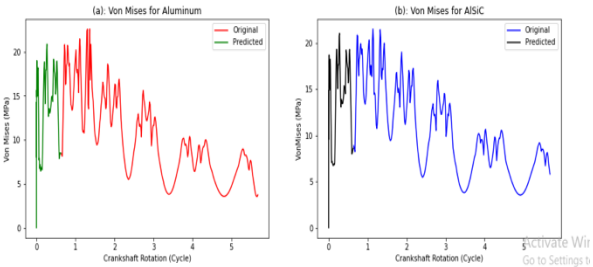

Fig. 11. Maximum stress produced in the connecting rod.

Figure 11 depicts the fluctuation of the maximum stress in the connecting rod throughout its operation. The piston is at the top dead center (TDC) when tensions on the connecting rod are at their highest. Maximum and minimum stresses per cycle range from 22MPa to 7MPa for Aluminum and Al-SiC, respectively. From the graph, it is observed that the relationship between the crankshaft rotation and the maximum stress of the connecting rod is a nonlinear relationship. The stress is more for both materials between the first two cycles and gradually drops thereafter.

The mechanical power created in each cylinder by the gas pressure is presented in Figure 12. It is worth noting that the power created is negative during the compression stroke before abruptly changing the sign during the combustion to become positive. The net mechanical power produced during a crankshaft rotation is the periodic average of the performance across a revolution.The mechanical power for cylinder 1, 2 and 4 reduces with the number of cycle with cylinder 3 being an exception as there was inconsistency in the mechanical power graph.

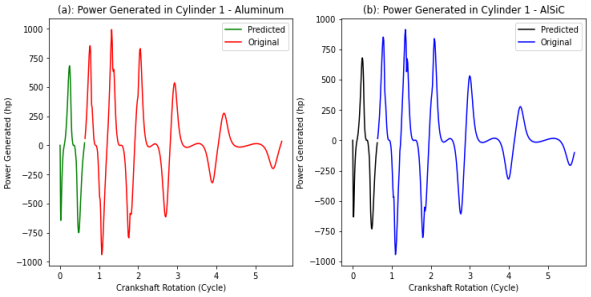

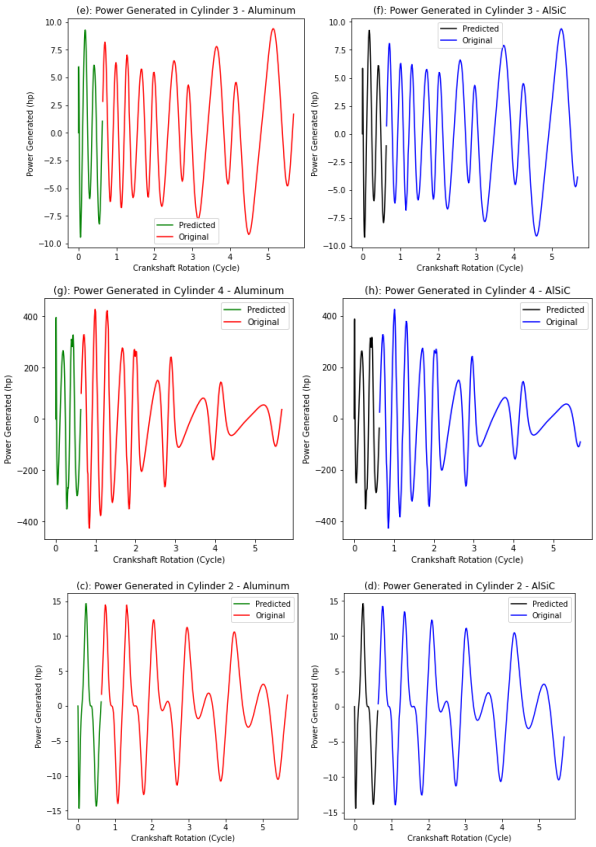

Fig. 12. Mechanical power generated in each cylinder.

Figure 13 displays the forces at the crankpin-to-connecting rod interface. In the z direction, the forces are most significant, whereas, in the y direction, they are almost negligible for both materials. These forces are greatest when the valve is very near to TDC. The connecting rod moves from a condition of compression to a state of tension throughout the operation, as evidenced by the change in sign of these forces. This just helps to highlight the importance of a suitable fatigue design.

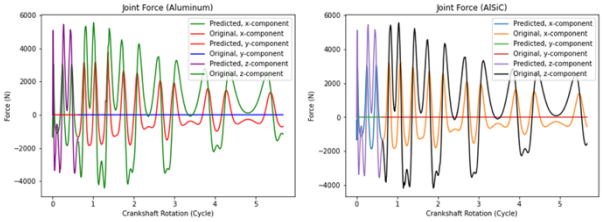

Fig. 13. Forces at the connecting rod and crankpin joint.

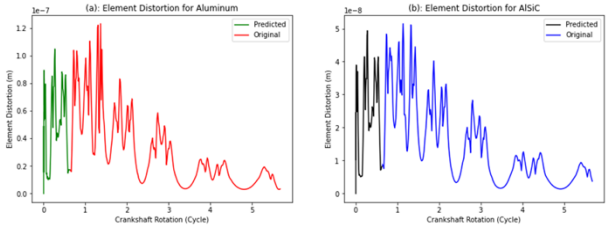

Fig. 14. Element distortion of the engine

The engine's overall element distortion is depicted in Figure 14. There is a surplus of Torque at the start of combustion; as the engine enters the power-producing phase of the operation, it establishes a positive engine distortion. Engine distortion is caused by the torque generated during expansion. Since gas torque directly affects the overall

engine torque, it is obvious that this is the primary process causing the engine distortion profile throughout the course of an engine cycle. From Figure 14, it is observed that AlSiC is less distorted, as compared to Aluminum which exhibits a greater element distortion. The distortion of both materials is more pronounced between the first two cycles and reduces drastically thereafter.

5. Conclusion

This study investigates the structural behavior of a connecting rod within a four-cylinder reciprocating engine, with a specific focus on the utilization of two distinct materials, namely aluminum and AlSiC. It is worth mentioning that the Von Mises stress experienced by AlSiC material is consistently lower than its yield strength, with a recorded value of around 5.5*M*Pa, in contrast to the yield strength of 43*M*Pa. In a similar vein, it can be seen that the Von Mises stress for Aluminum is roughly 3.5 *M*Pa, which is significantly lower than the yield strength of 276 *M*Pa. Both materials exhibited stress values that were below their respective yield strengths, therefore guaranteeing the structural integrity of the connecting rod. The study utilized a comprehensive technique that involved the integration of finite element analysis with the Autodesk Nastran solver® and Autodesk Fusion 360® software for simulation and modelling purposes.

The findings of the study suggest that both aluminum and AlSiC exhibit suitability as materials for internal combustion engines under the specific circumstances examined. Notably, aluminum demonstrates a lower level of stress, rendering it a preferable option for the connecting rod component. Furthermore, the examination brought attention to the I-section of the connecting rod as the primary locus of stress, underscoring the imperative for enhanced structural reinforcement in this specific location. The key component that influences the distortion profile and peak values of an engine is the engine torque.

The dependability and correctness of the model were proved by comparisons between simulation outputs and predicted values. Additionally, the safety of the redesigned design with respect to the chosen materials was confirmed by the finite element analysis. In general, the study highlights the practicality of utilizing aluminium and AlSiC to improve the structural integrity and functioning of engine components. The aforementioned discoveries enhance the comprehension of materials within the domain of engine engineering, hence facilitating the advancement of engines that are characterized by enhanced reliability and efficiency.

Furthermore, the results of this study possess the capacity to have a substantial influence on the progression of internal combustion engine technology. This influence may manifest in the development of engines that exhibit enhanced efficiency, durability, and reliability, thereby resulting in a reduction in the need for maintenance. The potential impact of these technical developments extends across other sectors, such as the automobile, aerospace, and marine industries, which significantly rely on internal combustion engines to power a wide range of applications and vehicles.

References

[1] K. R. Utsav, "Mathematical Modeling and Simulation of 3-Cylinder Engine," *Int. J. All Res. Educ. Sci. Methods (IJARESM)*, vol. 4, no. 7, pp. 62-66, Jul. 2016.

[2] F. Leach, G. Kalghatgi, R. Stone, and P. Miles, "The scope for improving the efficiency and environmental impact of internal combustion engines," *Transp. Eng.*, vol. 1, pp. 100005, Jun. 2020, doi:10.1016/j.treng.2020.100005.

[3] F. Parra, "Heat transfer investigations in a modern diesel engine," *Doctoral dissertation*, University of Bath, 2008.

[4] Z. Wang, X. Pan, W. Zhang, Y. Zhao, H. Li, and P. Liu, "The development trend of internal combustion engine," *in J. Phys.: Conference Series, IOP Publishing*, Oct. 2020, pp. 012139, doi:10.1088/1742-6596/1626/1/012139.

[5] L. Cozzi, "International EA, Gould T (International EA)," *World Energy Outlook*, vol. 2021, pp. 1–386, Oct. 2021.

[6] M. Briggs, J. Webb, and C. Wilson, "Automotive Modal Lock-in: The role of path dependence and large socio-economic regimes in market failure," *Econ Anal Policy*, vol. 45, pp. 58–68, Mar. 2015, doi:10.1016/j.eap.2015.01.005.

[7] G. Kalghatgi, "Is it really the end of internal combustion engines and petroleum in transport?," *Appl. Energy*, vol. 225, pp. 965–974, Sep. 2018, doi:10.1016/j.apenergy.2018.05.076.

[8] G. Kalghatgi, "Development of fuel/engine systems—the way forward to sustainable transport," *Eng.*, vol. 5, no. 3, pp. 510–518, Jun. 2019, doi:10.1016/j.eng.2019.01.009.

[9] B. Sudret, S. Marelli, and J. Wiart, "Surrogate models for uncertainty quantification: An overview," *2017 11th European conference on antennas and propagation (EUCAP)*, IEEE, pp. 793–797, Mar. 2017, doi:10.23919/EuCAP.2017.7928679.

[10] K. Cheng, Z. Lu, C. Ling, and S. Zhou, "Surrogate-assisted global sensitivity analysis: an overview," *Struct. Multidiscip. Optim.*, vol. 61, pp. 1187–1213, Marc, 2020, doi:10.1007/s00158-019-02413-5.

[11] A. I. J. Forrester and A. J. Keane, "Recent advances in surrogate-based optimization," *Prog. Aerosp. Sci.*, vol. 45, no. 1–3, pp. 50–79, Jan. 2009, doi:10.1016/j.paerosci.2008.11.001

[12] H. Adeli and C. Yeh, "Perceptron learning in engineering design," *Comp.-Aided Civ. Infrastruct. Eng.*, vol. 4, no. 4, pp. 247–256, Dec. 1989, doi:10.1111/j.1467-8667.1989.tb00026.x.

[13] Y. Xie, M. Ebad Sichani, J. E. Padgett, and R. DesRoches, "The promise of implementing machine learning in earthquake engineering: A state-of-the-art review," *Earthquake Spectra*, vol. 36, no. 4, pp. 1769–1801, Nov. 2020, doi:10.1177/8755293020919419.

[14] M. Flah, I. Nunez, W. Ben Chaabene, and M. L. Nehdi, "Machine learning algorithms in civil structural health monitoring: a systematic review," *Arch. Comput. Meth. Eng.*, vol. 28, pp. 2621–2643, Jun. 2021, doi:10.1007/s11831-020-09471-9.

[15] T. D. Akinosho, L. O. Oyedele, M. Bilal, A. O. Ajayi, M. D. Delgado, O. O. Akinade, and Ahmed, A.A., "Deep learning in the construction industry: A review of present status and future innovations," *J. Build. Eng.*, vol. 32, pp. 101827, Nov. 2020, doi:10.1016/j.jobe.2020.101827.

[16] G. Toh and J. Park, "Review of vibration-based structural health monitoring using deep learning," *Appl. Sci.*, vol. 10, no. 5, pp. 1680, Mar. 2020, doi:10.3390/app10051680.

[17] O. Avci, O. Abdeljaber, S. Kiranyaz, M. Hussein, M. Gabbouj, and D. J. Inman, "A review of vibration-based damage detection in civil structures: From traditional methods to Machine Learning and Deep Learning applications," *Mech. Syst. Signal Proc.*, vol. 147, p. 107077, Jan. 2021, doi:10.1016/j.ymssp.2020.107077.

[18] J. Dahlström, "Experimental Investigations of Combustion Chamber Heat Transfer in a Light-Duty Diesel Engine," *Doctoral Thesis*, Lund University, 2016.

[19] O. K. Adesina, A. I. Olanrewaju, and F. K. Abolanle, "Numerical Simulation and Modeling of UNSA91060 for Heat Transfer in Four-Stroke ICE Cylinder Head," *Int. J. Adv. Eng., Manag. Sci. (IJAEMS)*, pp.135-140, Jan. 2018, doi:10.22161/ijaems.4.3.1.

[20] M. Martins and H. Zhao, "Performance and emissions of a 4-cylinder gasoline engine with Controlled Auto-Ignition," *J. Brazilian Soc. Mech. Sci. Eng.*, vol. 34, pp. 436–440, Dec. 2012, doi:10.1590/S1678-58782012000400003.

[21] C. C. Xu and H. M. Choa, "The Analysis of the CFD about the Swirl Generation in Four-Stroke Engine," *Int. J. Appl. Eng. Res.*, vol. 11, no. 16, pp. 8940–8945, Jul. 2016.

[22] X. Cheng, X. Wang, Y. Ming, Z. Hongfei, and R. Gao, "Thermal-Mechanical Fatigue Analysis of Diesel Engine Cylinder Head Based on Fluid-Structure Interaction," *SAE Technical Paper 2015-01-0558*, Apr. 2015, doi:10.4271/2015-01-0558.

[23] M. J. Meman, A. B. Solanki, and A. J. Parmar, "Design, Modeling and Analysis of Structural Strength of Cylinder and Cylinder Head of 4-stroke (10 HP) CI Engine-A Review," *Int. J. Adv. Eng., Manag. Sci.*, vol. 2, no. 4, pp. 239409, Apr. 2016.

[24] D. B. Oke, I. O. Alabi, and A. A. Adegbola, "Heat Transfer Analysis in Internal Combustion Engine Piston Using Comsol Multiphysics: A Case Study of Tri-Cycle," *Int. J. Sci. & Eng. Res.*, vol. 7, no. 7, pp. 59-64, Jul. 2016.

[25] D. Karayel and V. Yegin, "Design and prototype manufacturing of a torque measurement system," *Acta Phys. Pol. A*, vol. 130, no. 1, pp. 272–275, Jul. 2016, doi:10.12693/APhysPolA.130.272.

[26] J. Agboola, T. Lebele-alawa, and B. Nkoi, "Study of combustion temperature distribution In the cylinder of compression ignition engine," *American J. Eng. Res.*, vol. 7, no. 11, pp. 304–312, Nov. 2018.

[27] E. Selmani, C. Delprete, and A. Bisha, "Cylinder liner deformation orders and efficiency of a piston ring-pack," *E3S Web of Conferences*, vol. 95, no. 1, pp. 04001, Jan. 2019, doi:10.1051/e3sconf/20199504001.

[28] A. Alshwawra, H. Pasligh, H. Hansen, and F. Dinkelacker, "Increasing the roundness of deformed cylinder liner in internal combustion engines by using a non-circular liner profile," *Int. J. Eng. Res.*, vol. 22, no. 4, pp. 1214–1221, Apr. 2021, doi:10.1177/1468087419893897.

[29] A. Alshwawra, F. Pohlmann-Tasche, F. Stelljes, and F. Dinkelacker, "Enhancing the Geometrical Performance Using Initially Conical Cylinder Liner in Internal Combustion Engines—A Numerical Study," *Appl. Sci.*, vol. 10, no. 11, pp. 3705, May 2020, doi:10.3390/app10113705.

[30] X. Zhu, Y. Cheng, and L. Wang, "Study on Deformation Characteristics of Diesel Engine Cylinder Liner under Different Influencing Factors," *in J. Phys.: Conference Series, IOP Publishing*, pp. 032019, Apr. 2021, doi:10.1088/1742-6596/1885/3/032019.

[31] J. Ž. Dorić and I. J. Klinar, "Efficiency of a new internal combustion engine concept with variable piston motion," *Therm. Sci.*, vol. 18, no. 1, pp. 113–127, Jan. 2014, doi:10.2298/TSCI110923020D.

[32] J. Popelka, "Measurement of the Torque of an Internal Combustion Engine Using Equipment of Our Own Design," *Int. J. Mech. Eng. Rob. Res.*, vol. 9, no. 1, pp. 66–70, Jan. 2020, doi:10.18178/ijmerr.9.1.66-70.

[33] A. Mogra and K. K. Gupta, "A Review on New Technology in Internal Combustion Engine-HCCI engine," *IOP Conference Series: Mat. Sci. Eng., IOP Publishing*, pp. 012054, Mar. 2020, doi:10.1088/1757-899X/810/1/012054.

[34] Z. J. Sroka, "Work Cycle of Internal Combustion Engine Due to Rightsizing," *Internal Combustion Eng. Techn. Appl. Biod. Fuel*, pp. 3, Aug. 2021, doi:10.5772/intechopen.97144.

[35] A. Atre, A. Bhorde, M. R. Khodke, D. Bhabad, and V. Aher, "Design and Buckling Analysis of Connecting Rod," *Int. J. Eng. Res. & Techn. (IJERT)*, vol. 10, no. 5, pp. 522–528, May 2021, doi:10.17577/IJERTV10IS050310.

[36] V. C. Pathade, B. Patle, and A. N. Ingale, "Stress analysis of IC engine connecting rod by FEM," *Int. J. Eng. Innovat. Techn.*, vol. 1, no. 3, pp. 12–15, Mar. 2012.

[37] K. Sreeraj Nair, K. Robert, and M. Shamnadh, "Static stress analysis of IC Engine cylinder head," *Int. Rev. Appl. Eng. Res.*, vol. 4, no. 2, pp. 123-128, 2014.

[38] S. Sathishkumara, M. Kannanb, and R. L. Sankarlalc, "Thermal Stress Analysis of Integrated combustion Engine Piston Using CAE Tools (Aluminum Silicon Alloy, Aluminum Silicon Alloy Steel)," *Acta Mech. Malays.* (AMM), vol. 3, no. 1, pp. 20–23, Jun. 2020, doi:10.26480/amm.01.2020.20.23.

[39] S. D. Kumar, T. Kasirajan, and C. S. Senthil, "Study on Structural Analysis of Connecting Rod and Crank Shaft Bearings," *Int. J. Appl. Eng. Res.*, vol. 10, no. 93, 2015.

[40] Q. Huang, "Application of artificial intelligence in mechanical engineering," *in 2nd International conference on computer engineering, information science & application technology* (ICCIA 2017), Atlantis Press, pp. 882–887, Jan. 2017, doi:10.2991/iccia-17.2017.154.

[41] A. Siddique, G. S. Yadava, and B. Singh, "Applications of artificial intelligence techniques for induction machine stator fault diagnostics," *4th IEEE International Symposium on Diagnostics for Electric Machines, Power Electronics and Drives, 2003. SDEMPED 2003, IEEE*, pp. 29–34, Sep. 2003, doi:10.1109/DEMPED.2003.1234543.

[42] L. B. Jack and A. K. Nandi, "Fault detection using support vector machines and artificial neural networks, augmented by genetic algorithms," *Mech Syst Sign. Proc.*, vol. 16, no. 2–3, pp. 373–390, Mar. 2002, doi:10.1006/mssp.2001.1454.

[43] H. Yang, J. Mathew, and L. Ma, "Intelligent diagnosis of rotating machinery faults-a review," *Proceedings of the 3rd Asia-Pacific Conference on System Integrity and Maintenance*, pp. 385-392, Sep. 2002.

[44] A. N. Bhatt and N. Shrivastava, "Application of artificial neural network for internal combustion engines: a state-of-the-art review," *Arch. Comp. Meth. Eng.*, vol. 29, no. 2, pp. 897–919, Mar. 2022, doi:10.1007/s11831-021-09596-5.

[45] N. K. Geetha and P. Bridjesh, "Overview of machine learning and its adaptability in mechanical engineering," *Mater. Today Proc.*, Nov. 2020, doi:10.1016/j.matpr.2020.09.611.

[46] C. Wang, H. Fu, L. Jiang, D. Xue, and J. Xie, "A property-oriented design strategy for high performance copper alloys via machine learning," *NPJ. Comput. Mater.*, vol. 5, no. 1, pp. 87, Aug. 2019, doi:10.1038/s41524-019-0227-7.

[47] Z. Zhou, Y. Zhou, Q. He, Z. Ding, F. Li, and Y. Yang, "Machine learning guided appraisal and exploration of phase design for high entropy alloys," *NPJ. Comput. Mater*., vol. 5, no. 1, p. 128, Dec. 2019, doi:10.1038/s41524-019-0265-1.

[48] Y. Zhang, C. Wen, C. Wang, S. Antonov, D. Xue, Y. Bai, and Su, Y., "Phase prediction in high entropy alloys with a rational selection of materials descriptors and machine learning models," *Acta Mater*., vol. 185, pp. 528–539, Feb. 2020, doi:10.1016/j.actamat.2019.11.067.

[49] N. Islam, W. Huang, and H. L. Zhuang, "Machine learning for phase selection in multi-principal element alloys," *Comp. Mat. Sci.*, vol. 150, pp. 230–235, Jul. 2018, doi: 10.1016/j.commatsci.2018.04.003.

[50] L. Ward, S. C. O'Keeffe, J. Stevick, G. R. Jelbert, M. Aykol, and C. Wolverton, "A machine learning approach for engineering bulk metallic glass alloys," *Acta Mater.,* vol. 159, pp. 102–111, Oct. 2018, doi: 10.1016/j.actamat.2018.08.002.

[51] C. Wen, Y. Zhang, C. Wang, D. Xue, Y. Bai, S. Antonov, L. Dai, T. Lookman, and Su, Y., "Machine learning assisted design of high entropy alloys with desired property," *Acta Mater.*, vol. 170, pp. 109–117, May 2019, doi:10.1016/j.actamat.2019.03.010.

[52] G. Kim, H. Diao, C. Lee , A. T. Samaei, T. Phan, M. de Jong, K. An, D. Ma, P. K. Liaw, W. Chen, "First-principles and machine learning predictions of elasticity in severely lattice-distorted high-entropy alloys with experimental validation," *Acta Mater.*, vol. 181, pp. 124–138, Dec. 2019, doi:10.1016/j.actamat.2019.09.026.

[53] *Fusion 360 | 3D CAD, CAM, CAE, & PCB Cloud-Based Software | Autodesk*. Autodesk Fusion 360: More than CAD, it's the future of design and manufacturing, Accessed: May 20, 2023. [Online]. Available: https://www.autodesk.com/products/fusion-360/overview?term=1-YEAR&tab=subscription

[54] *Autodesk Inventor Nastran | IMAGINiT*. CAD-embedded FEA, Accessed: May 20, 2023. [Online]. Available: https://www.imaginit.com/software/autodesk-products/nastran-in-cad

[55] L. F. da Silva, R. D. Adams, C. Sato, and K. Dilger, "Applications of adhesive bonding," *Proceedings of the Institution of Mechanical Engineers, Part D: J. of Automobile Eng*., SAGE Publications, vol. 237, no. 13, pp. 2975-2975, Nov. 2023, doi:10.1177/09544070231185666.